Exp. Theo. NANOTECHNOLOGY 3 (2019) 405-426 https://doi.org/10.56053/3.3.405

Natural convection in inclined channel for air cooling of photovoltaic panels

A. H. Laatar[1,2-*], *S. Kennich*[2,3], *J. Balti*[3], *N. Badi*[1]

[1] Department of Physics, Renewable Energy Laboratory, University of Tabuk, Tabuk 71491, Kingdom of Saudi Arabia
[2] LETTM, Faculty of Mathematical, Physical and Natural Sciences of Tunis, University of Tunis El Manar, 2092- Tunis, Tunisia
[3] Faculty of Sciences of Bizerte, University of Carthage, 7021- Jarzouna, Tunisia
*) Email: ahlaatar@gmail.com

Received 14/12/2018, *Accepted* 28/6/2019, *Published* 15/9/2019

Reducing the operating temperature of a photovoltaic (PV) module is an effective way to improve efficiency and prevent damage from overheating. The present paper focuses on the study of the effect of inclination on air natural convection in an asymmetrically heated channel (at uniform heat flux), in laminar regime. This configureuration models the passive and natural air-cooling of PV panels by inclined chimneys. The computational procedure solves the unsteady two-dimensional Navier-Stokes and energy equations by a finite volume approach while the projection method decouples the pressure from the velocity. The heat transfer and fluid flow are analyzed for a wide range of modified Rayleigh numbers varying from 10^2 to 10^5 and for inclination angles between 15^o and 90^o with respect to horizontal position. The results show that the mass flow rate and the average Nusselt number increase with the angle of inclination as well as with the modified Rayleigh number. However, a significant reduction in heat transfer rate and induced flow rate is observed for the low angles of inclination. To enhance the cooling of the PV panel, extensions are added at the inlet and outlet of the channel. The simulations show that only the downstream extensions of the channel are effective in improving the induced mass flow rate and therefore the convective heat transfer.

Keywords: PVs; Analysis; Characterization.

Exp. Theo. NANOTECHNOLOGY 3 (2019) 405-426

1. INTRODUCTION

Many countries around the world have great potential in solar energy, which allows them to produce large quantities of electricity using photovoltaic cells (PV cells). However, in these hot and dry regions, daytime temperatures can reach extreme values, which will drastically reduce the efficiency of PV panels and cause long-term damage. These problems can be avoided by external cooling system that can help maintaining the PV panel temperature within the working range and thus improve the efficiency. Based on these considerations, the efficiency and the life of the solar panels can be improved by maintaining their operating temperatures as low as possible. Several cooling techniques have been proposed in the literature, mostly based on water and air-cooling, as these are the simplest techniques. The literature also shows other types of more sophisticated cooling mechanisms for PV panels as immersion cooling, heat pipes, microchannels, impingements jet, phase change material cooling, heat sinks and improved heat exchangers [1-4]. However, the cooling of PV panels requires a separate system that will eliminate excess heat, but the cost of manufacturing and maintaining this system may outweigh the benefits of improving electrical efficiency. Cooling methods can be classified into two categories: active methods, which consume energy (fan, pump, etc.) and passive methods, which use natural convection or conduction to extract heat. Active cooling techniques are generally more efficient than passive ones. However, in many cases, passive cooling can be an interesting solution given its low cost. Most of these methods are based on air or water-cooling. In desert regions, water is scarce and therefore air-cooling techniques become necessary, despite their low efficiency. Passive systems based on natural convection in vertical or inclined channels are used in many technological applications such as photovoltaic cooling systems, solar collectors and passive ventilation of buildings. In the literature, many recent papers have been interested in such configureurations, both from the experimental point of view [5-7], and from the analytical or numerical point of view [8-12], in the continuity of previous work during the last decades.

Passive cooling system using the natural draft of air has been previously suggested by (Tonui and Tripanagnostopoulos 2007 [13], and by Tonui and Tripanagnostopoulos 2008 [14], for cooling PV panels that are mounted on the roofs of houses. Natural convection in an inclined channel heated asymmetrically, can model this configureuration. In the past, numerous experimental and numerical studies have been carried out to understand the effect of inclination on the thermal performance of inclined channels [15-23].

In this study, we will examine how to use natural convection for cooling photovoltaic panels. In this work will be analyzed the idea of using an inclined chimney as a passive cooling system for photovoltaic cells without having recourse to the energy produced by the photovoltaic panel itself. The chimney is a rectangular duct covering the back of the panel and extending at the outlet of the channel. The added extensions allow to increase the draft of the chimney and consequently the improvement of the efficiency of the PV panel. The system is passive because the flow of air in the channel is entirely induced by buoyancy.

Exp. Theo. NANOTECHNOLOGY 3 (2019) 405-426

2. PROBLEM DESCRIPTION

Figure 1 schematically illustrates the physical problem under study. It consists of a two-dimensional open-ended inclined channel, asymmetrically heated by a constant heat flux q imposed on its top wall. The channel length is H whereas the plate-to-plate spacing (channel width) is b leading to an aspect ratio Ar = H/b. The channel is tilted by an angle ϕ with respect to the horizontal plane.

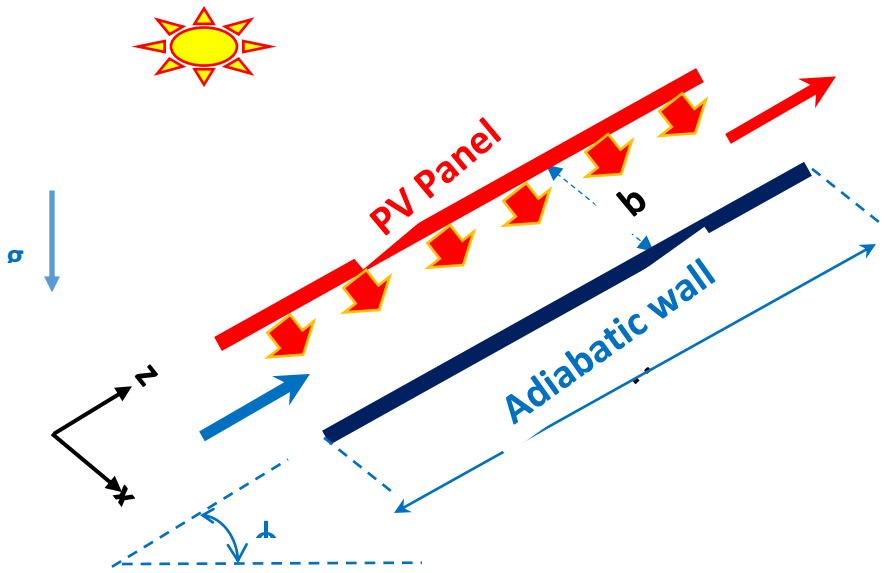

Figure 1: Geometrical configureuration in the case of a simple inclined channel.

The flow through the studied channel is induced entirely by buoyancy. All the thermophysical properties are assumed to be constant, except for the density in the buoyancy force term which can be modeled by Boussinesq approximation. The governing equations are the two-dimensional Navier-Stokes and energy equations written in dimensionless form as follows:

Under these assumptions the non-dimensional governing equations read:

$$\frac{\partial U}{\partial X}+\frac{\partial W}{\partial Z}=0 \tag{1}$$

$$\frac{\partial U}{\partial t}+U\frac{\partial U}{\partial X}+W\frac{\partial U}{\partial Z}=-\frac{\partial P}{\partial X}+Pr\left(\frac{\partial^2 U}{\partial X^2}+\frac{\partial^2 U}{\partial Z^2}\right)+Pr\,Ra\,cos\varphi\,T \tag{2}$$

$$\frac{\partial W}{\partial t}+U\frac{\partial W}{\partial X}+W\frac{\partial W}{\partial Z}=-\frac{\partial P}{\partial Z}+Pr\left(\frac{\partial^2 W}{\partial X^2}+\frac{\partial^2 W}{\partial Z^2}\right)+Pr\,Ra\,sin\varphi\,T \tag{3}$$

$$\frac{\partial T}{\partial t}+U\frac{\partial T}{\partial X}+W\frac{\partial T}{\partial Z}=\left(\frac{\partial^2 T}{\partial X^2}+\frac{\partial^2 T}{\partial Z^2}\right) \tag{4}$$

Exp. Theo. NANOTECHNOLOGY 3 (2019) 405-426

The dimensionless variables are defined as follows:

$$(X, Z) = \frac{(x,z)}{b} \quad (5) \qquad t = \frac{\alpha t'}{b^2} \quad (6)$$

$$(U, W) = \frac{(u,w)b}{\alpha} \quad (7) \qquad T = \frac{\theta - \theta_0}{(qb/\lambda)} \quad (8)$$

The governing dimensionless parameters appearing in the above equations are the Rayleigh number (9) and the Prandtl number (10):

$$Ra = \frac{g\beta q b^4}{\lambda \alpha \nu} \quad (9)$$

$$Pr = \frac{\nu}{\alpha} \quad (10)$$

In this study, we consider a computational domain restricted to the channel-chimney system geometry. The Navier-Stokes and energy equations are solved by imposing the boundary conditions given in the following:

On the heated wall of the channel:

$$U = W = 0 \; and \;\; \frac{\partial T}{\partial X} = -1 \quad (11)$$

On the unheated wall of the channel:

$$U = W = 0 \; and \;\; \frac{\partial T}{\partial X} = 0 \quad (12)$$

At the inlet of the channel:

$$\frac{\partial W}{\partial Z} = U = T = 0 \quad (13)$$

$$P = -0.5\left\{\int_0^1 W(X,0)dX\right\}^2 \quad (14)$$

At the outlet of the channel:

If $W \geq 0$

$$\frac{\partial W}{\partial Z} = \frac{\partial U}{\partial Z} = \frac{\partial T}{\partial Z} = P = 0 \quad (15)$$

Else

$$\frac{\partial W}{\partial Z} = U = T = 0 \quad (16)$$

$$P = -0.5\frac{1}{\Delta}\left\{\int_\Delta W(X,0)dX\right\}^2 \quad (17)$$

Δ is a length of the outlet section where the air is incoming into the chimney.

The above open boundary conditions (Eqs. 16-20) are identical to those proposed in [17, 18, 22].

Exp. Theo. NANOTECHNOLOGY 3 (2019) 405-426

The induced mass flow rate in the channel-chimney system is defined as:

$$G = \int_0^1 W(X,0)dX \tag{18}$$

The local Nusselt number over the heated wall of the channel can be evaluated from equation:

$$Nu(Z) = \frac{h(Z)b}{\lambda} = \frac{1}{T_w(Z)} \tag{19}$$

The heat transfer rate over the heated wall, is represented by the average Nusselt number, defined as:

$$Nu(Z) = \frac{1}{A_r}\int_0^{A_r} Nu(0,Z)dZ \tag{20}$$

3. NUMERICAL METHOD

The calculation has been performed using a time-dependent Navier-Stokes solver, which was initially developed at LIMSI (CNRS FRANCE). This software has successfully resolved different types of problems [24 - 27].

The conservation equations (1 - 4) are integrated by a finite volume approach and then solved in time using a prediction-projection algorithm, which allows one to decouple pressure from velocity.

Assuming all quantities known at time $n.\Delta t$ the solution at time $(n+1).\Delta t$ is obtained in three steps.

First, an intermediate velocity field V^* is first computed using a second-order time scheme. This time stepping combines a second order backward Euler scheme for the diffusion terms, with an explicit second-order Adams-Bashforth extrapolation for the non-linear terms, taking into consideration known pressure field. The formula used in this step reads:

$$\frac{3V^*-4V^n+V^{n+1}}{2\Delta t} + 2(V.\nabla V)^n - (V.\nabla V)^{n-1} = -\nabla P^n + Pr\Delta V^* \tag{21}$$

As for the second step, the intermediate velocity field is projected onto the subspace of divergence free vector field using the Helmholtz decomposition theorem:

$$V^{n+1} - V^* = -\frac{2\Delta t}{3}\nabla(P^{n+1} - P^n) \tag{22}$$

It is achieved by taking the divergence of equation giving rise to a Poisson's type equation for the incremental pressure:

$$\Delta\Psi = \frac{3}{2\Delta t}\nabla V^* \;\; ; \;\; \Psi = P^{n+1} - P^n \tag{23}$$

The last equation is solved with a multigrid algorithm. The main idea of this algorithm is to accelerate the convergence of a basic iterative method by using grids of different mesh sizes ([27] and [28]).

When the pressure field is obtained, the new quantities at $(n+1).\Delta t$ are given by:

Exp. Theo. NANOTECHNOLOGY 3 (2019) 405-426

$$\begin{cases} P^{n+1} = \Psi + P^n \\ V^{n+1} = V^* - \frac{2\Delta t}{3}\nabla\Psi \end{cases} \quad (24)$$

The space discretization utilizes a centered scheme both for convective and diffusive terms.

The computations were performed on a 2D computational domain restricted to the space between channel plates. The computational domain is $[0,\ X_m] * [0, Z_m]$ where X_m=1 and Z_m=H/b= 5.

The spatial discretization used was a non-uniform grid in the wall normal direction and a uniform grid in stream-wise direction. The refinement is near the channel walls.

In order to ensure the accuracy of the numerical results, a grid dependence study was realized for the vertical channel. Computations were carried out with different gridlines systems, i.e. 66*130, 66*258, 98*258, 130*258 and 98*514 with $Ra^*=10^5$. The last three gridlines systems give errors less than 1.5% in the relevant parameters such as the mass flow rate and the average Nusselt number. Therefore, 98*258 gridlines system is suitable and used throughout the present work. The time step is fixed at $\Delta t= 10^{-5}$, close to the stability limit.

4. VALIDATION OF THE MODEL

In order to validate our numerical model, comparisons with results available in the literature were performed.

The first validation concerns a comparison with the experimental results of Webb and Hill [28] for the vertical channel. Figure 2 shows the average Nusselt number as a function of the modified Rayleigh number in the case of a vertical channel (Ar= H/b =5 and $\phi=90^o$). It is clear that the values of the average Nusselt number obtained numerically in the present work are in better agreement with the correlation given in [28].

Exp. Theo. NANOTECHNOLOGY 3 (2019) 405-426

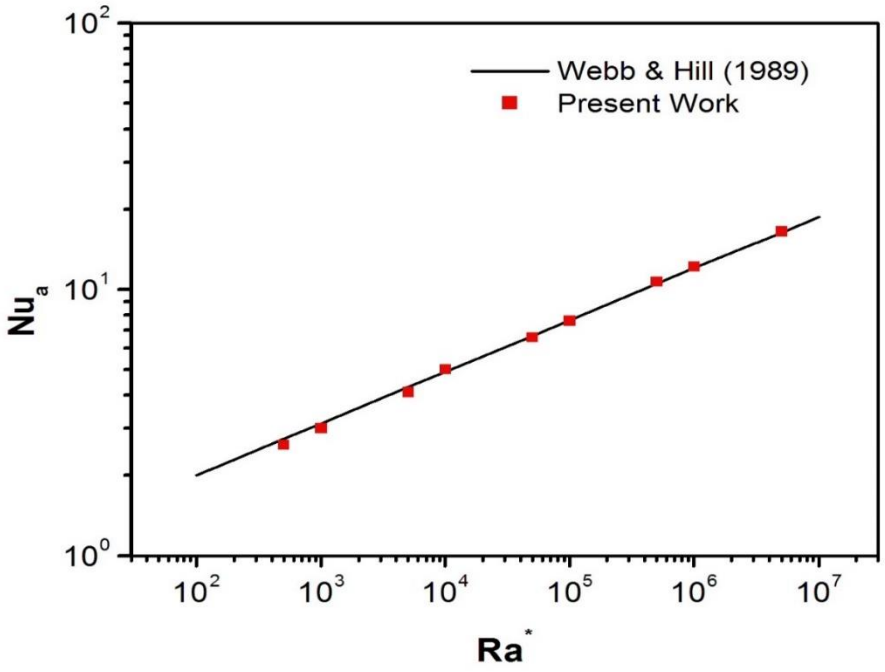

Figure 2 Average Nusselt number as a function of the modified Rayleigh number in the case of a vertical channel (A_r= H/b =5 and ϕ=90^o).

Exp. Theo. NANOTECHNOLOGY 3 (2019) 405-426

The second validation test uses the numerical results presented by Mittelman et al. [20] relating to the passive cooling of inclined photovoltaic panels. Figureure 3 depicts the variation of the average Nusselt number as a function of the modified Rayleigh number in the case of an inclined channel (Ar= H/b=30 and ϕ=30^o). As can be seen, our results are in perfect agreement with the correlations proposed by Mittelman et al. [20].

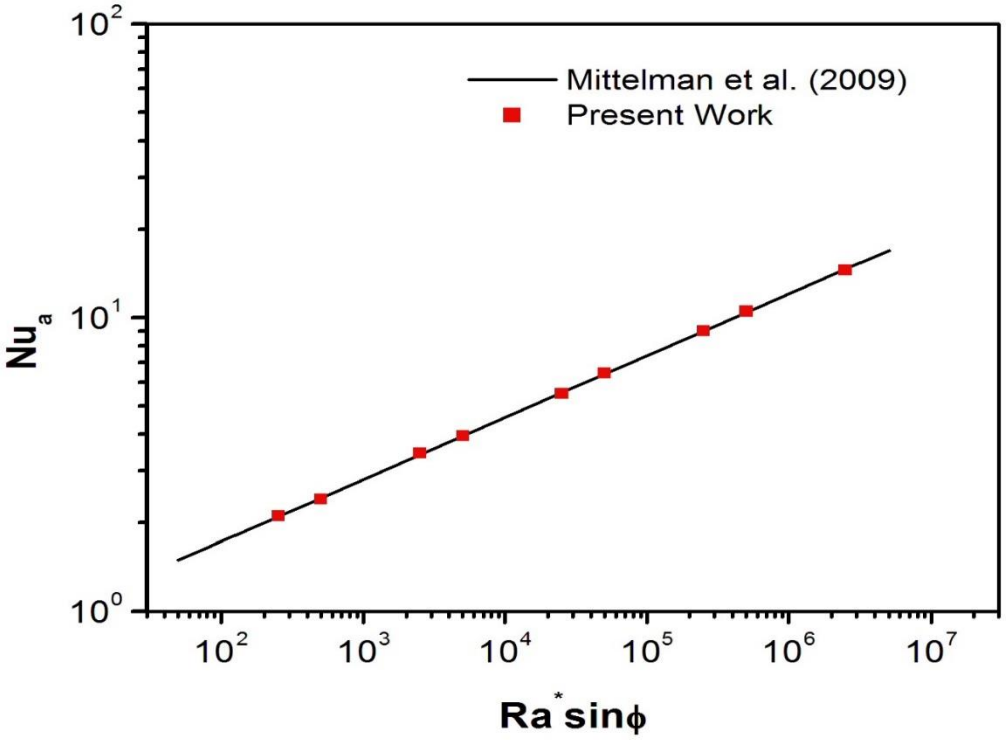

Figure 3 Average Nusselt number as a function of the modified Rayleigh number in the case of an inclined channel (A_r= H/b=30 and ϕ=30^o).

5. RESULTS AND DISCUSSION

The inclined open channel for the air-cooling of PV panels is schematically illustrated in Figure 1. The channel is formed of two parallel plates of length H whereas the plate-to-plate spacing is b (channel width) leading to an aspect ratio A_r = H/b. The upper wall consists of the PV panel while the lower part consists of an adiabatic plate. The channel is tilted by an angle ϕ with respect to the horizontal plane.

The effect of inclination on air natural convection in an asymmetrically heated channel will be studied in laminar regime. In the following, the configureuration of the channel without adiabatic extensions will be called a simple channel. The study covers a wide range of angle of inclination ($15\ ^\circ \leq \phi \leq 90\ ^\circ$) and modified Rayleigh number ($10^2 \leq Ra^* \leq 10^5$). The calculations will be

Exp. Theo. NANOTECHNOLOGY 3 (2019) 405-426

performed for a channel aspect ratio A_r = 5, the same as that of the Webb and Hill experiment (1989). This choice was also made on the basis of the abundance of results relating to this aspect ratio in the literature. It should be noted that Talukdar et al. [29] have conducted a numerical study to predict the optimum aspect ratio that maximizes the heat transfer rate in vertical channel with large temperature difference, under non-Boussinesq approximation and with temperature dependent fluid properties. They found that the optimal aspect ratio decreases with increasing Rayleigh number.

5.1 Simple channel case

At first, we will be interested in the case of the simple channel (without extensions) which will be the basic case. For this, we will study the effect of inclination on natural convection in an asymmetrically heated inclined channel. We will discuss more particularly the effect of tilt angle on heat transfer rate and mass flow rate for a range of modified Rayleigh number from 10^2 to 10^5, while keeping the other parameters fixed. Figure 4 shows the variation of the dimensionless mass flow rate as a function of the angle of inclination for different modified Rayleigh numbers in the case of a simple tilted channel. It is seen that curves have the same shape. It is observed that the mass flow rate induced by chimney effect increases with the increase of the inclination angle and the modified Rayleigh number. It should be noted that significant reductions in air flow rate are noted for low angles of inclination, beyond 30^o.

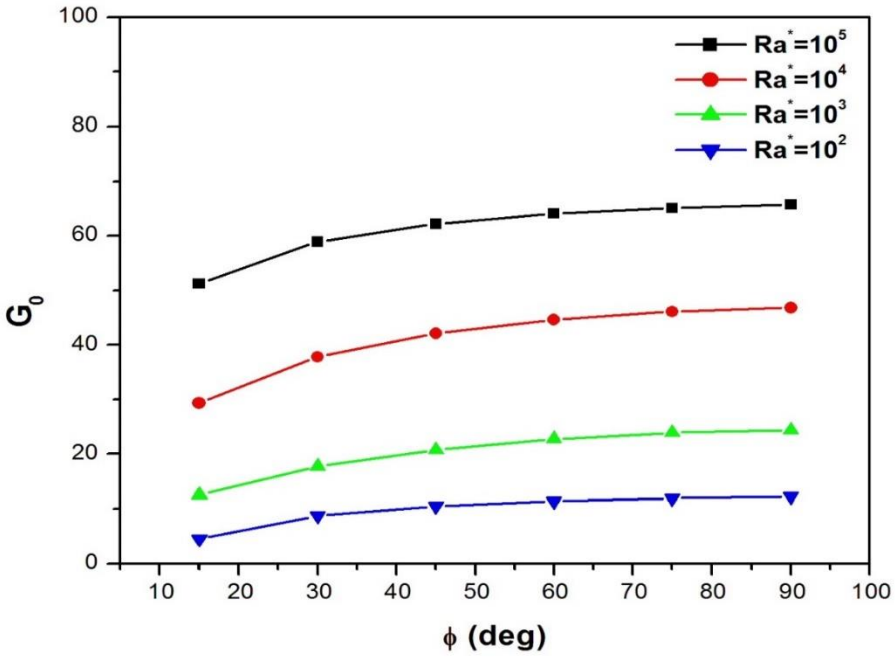

Figure 4 Dimensionless mass flow rate as a function of the angle of inclination for different modified Rayleigh numbers in the case of a simple tilted channel (A_r= H/b=5).

Exp. Theo. NANOTECHNOLOGY 3 (2019) 405-426

Figure 5 displays the variation of the average Nusselt number as a function of the angle of inclination for various modified Rayleigh numbers. It is observed that with the decrease of the angle of inclination from 90º to 15º the heat transfer rate decreases significantly with the decrease of the modified Rayleigh number, and more particularly for angles of inclination less than 30º.

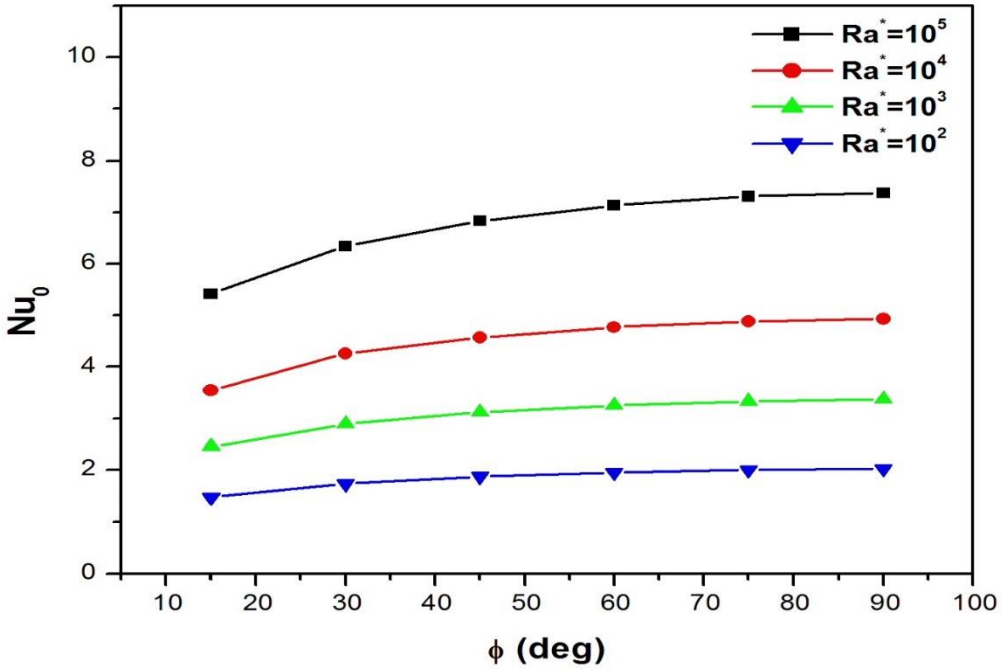

Figure. 5: Average Nusselt number as a function of the angle of inclination for different modified Rayleigh numbers in the case of a simple tilted channel (A_r= H/b=5).

5.2 Channel with extensions

After studying the simple channel case, we introduce adiabatic extensions at the inlet and outlet of the simple channel in order to improve both heat transfer and the mass flow rate induced by buoyancy. Figure 6 schematically shows the geometric configureuration of the inclined channel with adiabatic extensions of lengths E_{in} and E_{out}. In the following, we will keep the same aspect ratio for the simple channel (A_r = H / b = 5). Then, we will add extensions of the same length (E_{in} = E_{out} = H/2) as in the Webb and Hill experiment (1989). To test the utility of the extensions, three geometric configureurations will be studied. The first one is that of the simple channel with two extensions at the input and the output (E_{in} = E_{out} = H/2). In the second test, we keep the extension at the entrance and we eliminate the one at the exit (E_{in} = H/2, E_{out} = 0). For the third configureuration, we eliminate the extension at the entry and we keep the one at the exit (E_{in}=0, E_{out} = H/2).

Exp. Theo. NANOTECHNOLOGY 3 (2019) 405-426

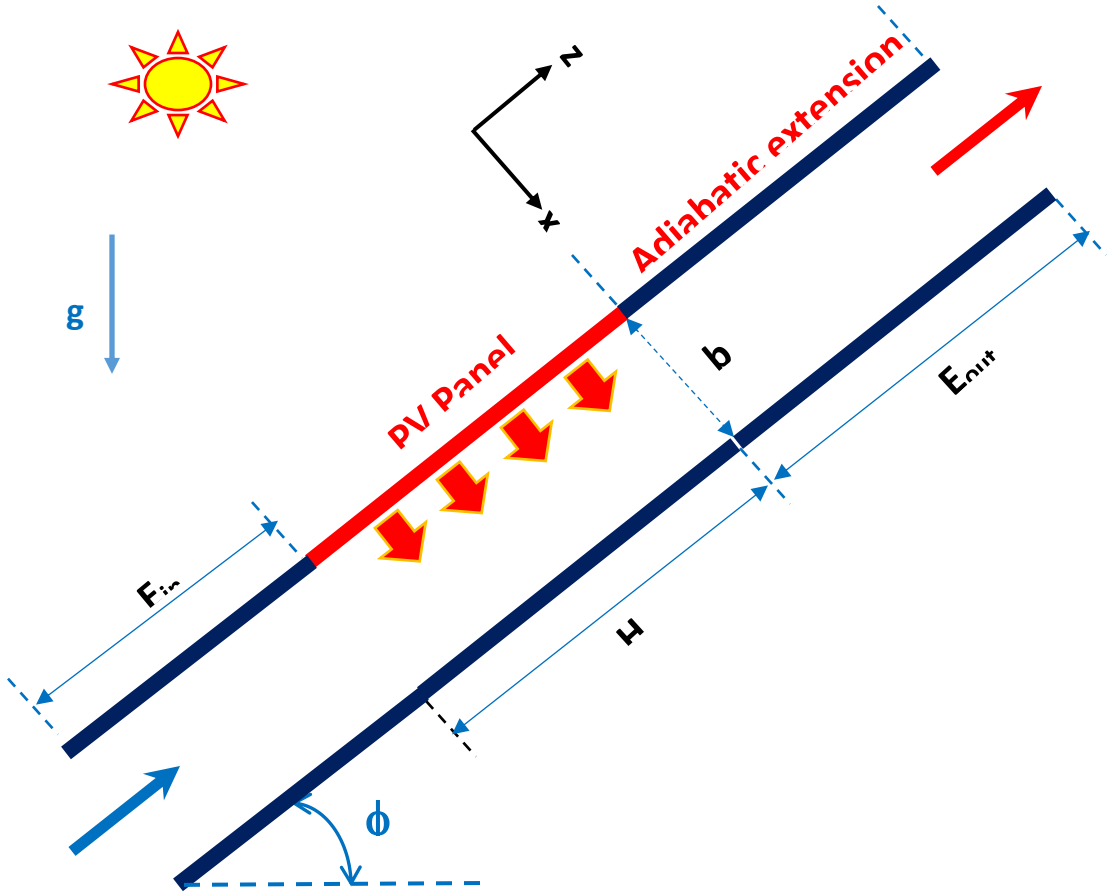

Figure 6 Geometrical configuration in the case of an inclined channel with adiabatic extensions.

To quantify in a concise way the improvement of the mass flow rate and the convective heat transfer with respect to the simple channel, two ratios G/G_0 and Nu/Nu_0 are introduced. These two quantities represent the dimensionless mass flow rate G and the average Nusselt number Nu of the modified channel, normalized by those of the simple channel (G_0 and Nu_0) for the same parameters. The first set of results pertains to the effect of the inclination angle on the ratios G/G_0 and Nu/Nu_0. Figure 7 shows the variation of the ratio G/G_0 as a function of the angle of inclination f for various modified Rayleigh numbers and for the three test cases related to extensions.

Exp. Theo. NANOTECHNOLOGY 3 (2019) 405-426

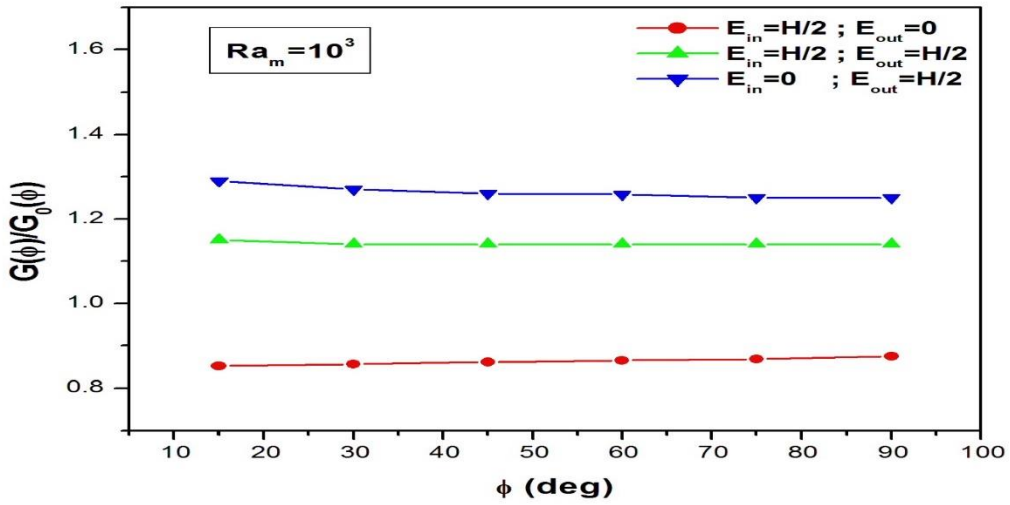

Figure 7a: Variation of the ratio G/G_0 as a function of the angle of inclination for different adiabatic extensions at the inlet and the outlet of the channel ($Ra^*=10^3$).

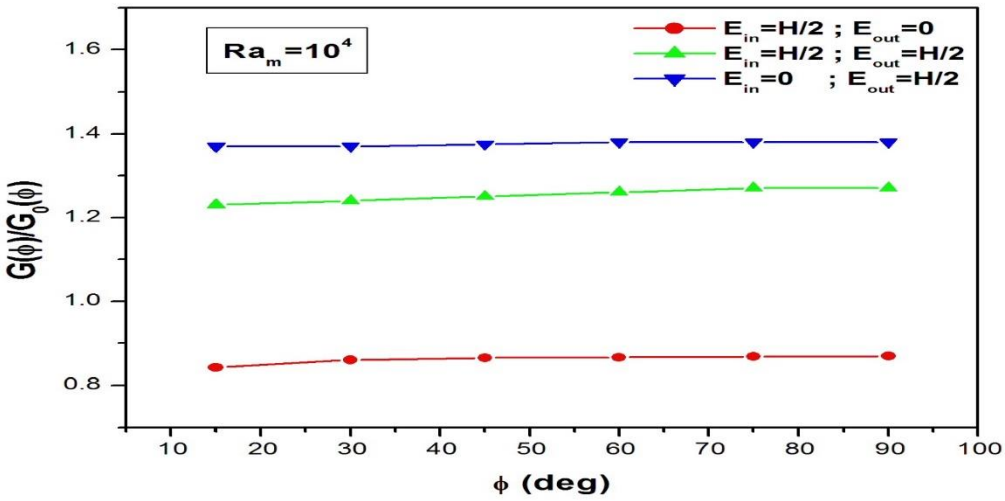

Figure 7b: Variation of the ratio G/G_0 as a function of the angle of inclination for different adiabatic extensions at the inlet and the outlet of the channel ($Ra^*=10^4$).

Exp. Theo. NANOTECHNOLOGY 3 (2019) 405-426

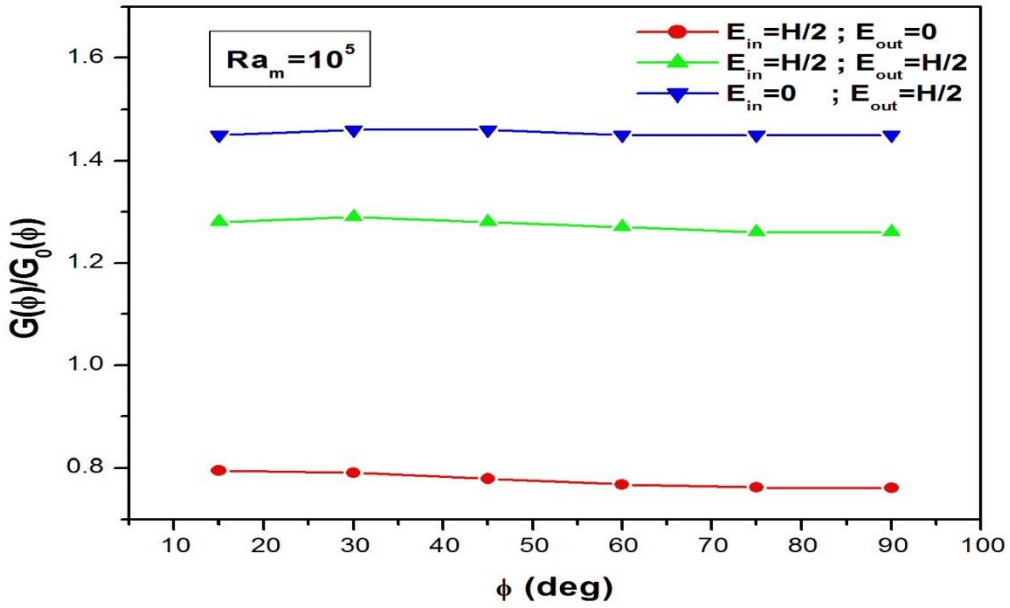

Figure 7c: Variation of the ratio G/G_0 as a function of the angle of inclination for different adiabatic extensions at the inlet and the outlet of the channel ($Ra^*=10^5$).

The introduction of the extension only at the channel inlet (E_{in} = H/2, E_{out} = 0) does not improve the mass flow rate for all modified Rayleigh numbers ($Ra^*=10^3$, 10^4, 10^5) and for all inclination angles ($15° \leq \phi \leq 90°$) considered in this study, since the ratio G/G0 is always less than 1. This configuration is the most unfavorable among the three tests. It reduces the mass flow by more than 20% for all inclination angles, when the modified Rayleigh number is equal to 10^5. The most interesting configuration is that of introducing an extension only at the outlet of the channel (E_{in}=0, E_{out} = H/2). It improves the mass flow rate by more than 45% for all tilt angles, when the modified Rayleigh number is 10^5.

The variation of the ratio Nu/Nu_0 as a function of the angle of inclination for different modified Rayleigh numbers and for the three test cases is reported in Figure 8. Among the three cases studied, only the configuration where the extension is added to the outlet of the channel (E_{in}=0, E_{out} = H/2) improves the heat transfer rate at the heated wall. For all modified Rayleigh numbers ($Ra^*=10^3$, 10^4,10^5) and for all inclination angles ($15° \leq \phi \leq 90°$) considered in this study, the ratio Nu/Nu0 is always greater than 1. This configuration allows an improvement in the heat transfer rate of 5% on average. For low inclinations and low Rayleigh numbers, a rate of 9% can be achieved. In conclusion, the extensions at the inlet of the channel are to be eliminated and only extensions at the channel outlet should be added to improve both the mean Nusselt number and the mass flow rate.

Exp. Theo. NANOTECHNOLOGY 3 (2019) 405-426

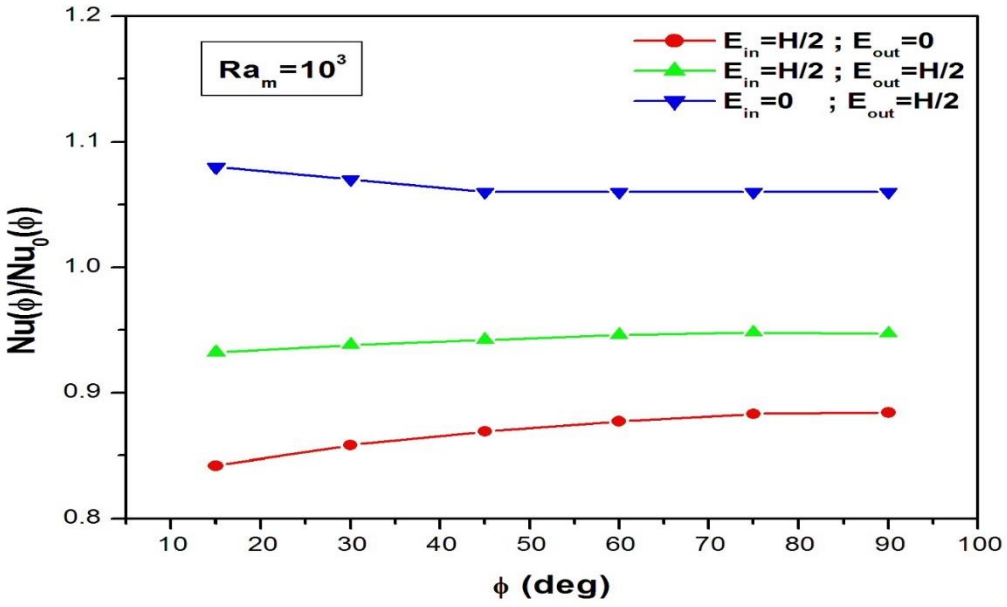

Figure 8a Variation of the ratio Nu/Nu_0 as a function of the angle of inclination for different adiabatic extensions at the inlet and the outlet of the channel ($Ra^*=10^3$).

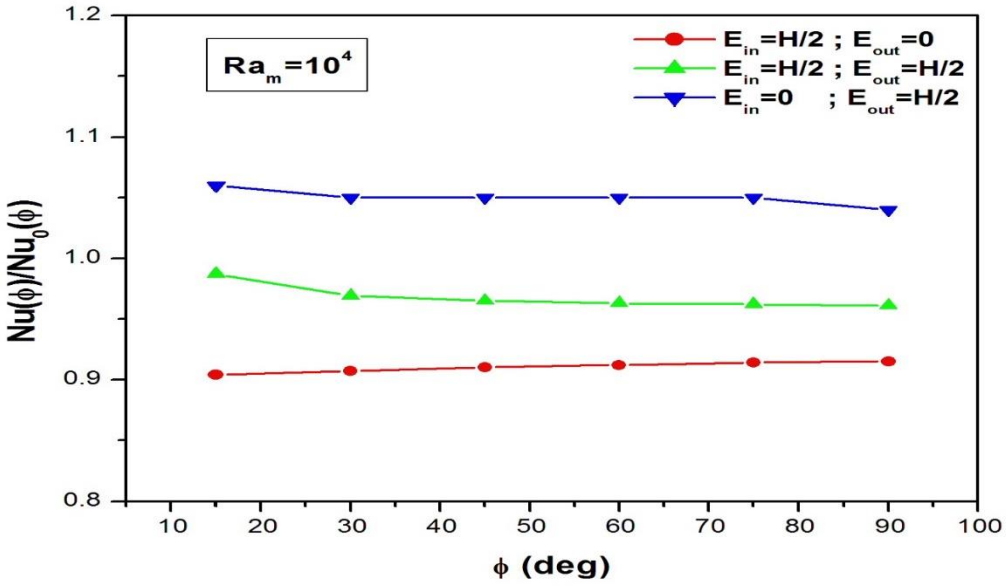

Figure 8b Variation of the ratio Nu/Nu_0 as a function of the angle of inclination for different adiabatic extensions at the inlet and the outlet of the channel ($Ra^*=10^4$).

Exp. Theo. NANOTECHNOLOGY 3 (2019) 405-426

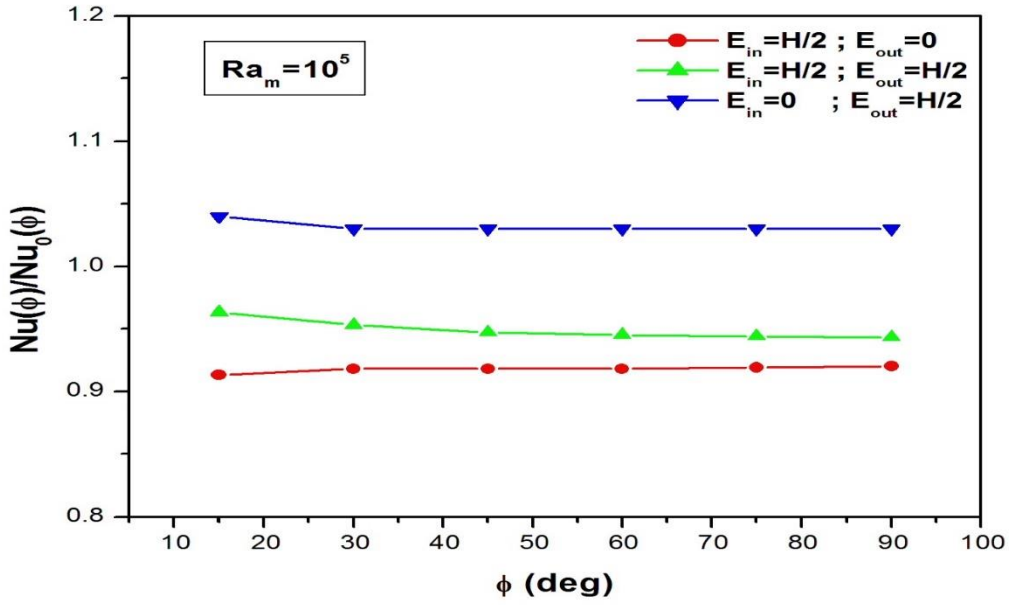

Figure 8c Variation of the ratio Nu/Nu_0 as a function of the angle of inclination for different adiabatic extensions at the inlet and the outlet of the channel ($Ra^*=10^5$).

To explain the heat transfer rate improvement for this best configuration ($E_{in}=0$, $E_{out}=H/2$), Figure 9 shows the streamlines and the temperature fields for different inclination angles and for a modified Rayleigh number $Ra^*=10^5$. For high inclination angles ($60\ ° \leq \phi \leq 90\ °$), the flow becomes of the boundary layer type. Fluid along the boundary layer is accelerated along the heated wall. This convective layer is fed by both the fluid entering through the bottom of the channel and from the top through a reverse flow along the cold wall. At the channel exit, a recirculation zone adjacent to the cold wall appears. The size of this vortex is almost the same for high inclination angles ($60° \leq \phi \leq 90°$), which explains the small variation of the mass flow rate for these angles. For low inclination angles ($15° \leq \phi \leq 30°$), the size of the recirculation zone decreases and the convective layer becomes thicker. The fluid is then slowed, which explains the low thermal transfers for this range of inclination.

Exp. Theo. NANOTECHNOLOGY 3 (2019) 405-426

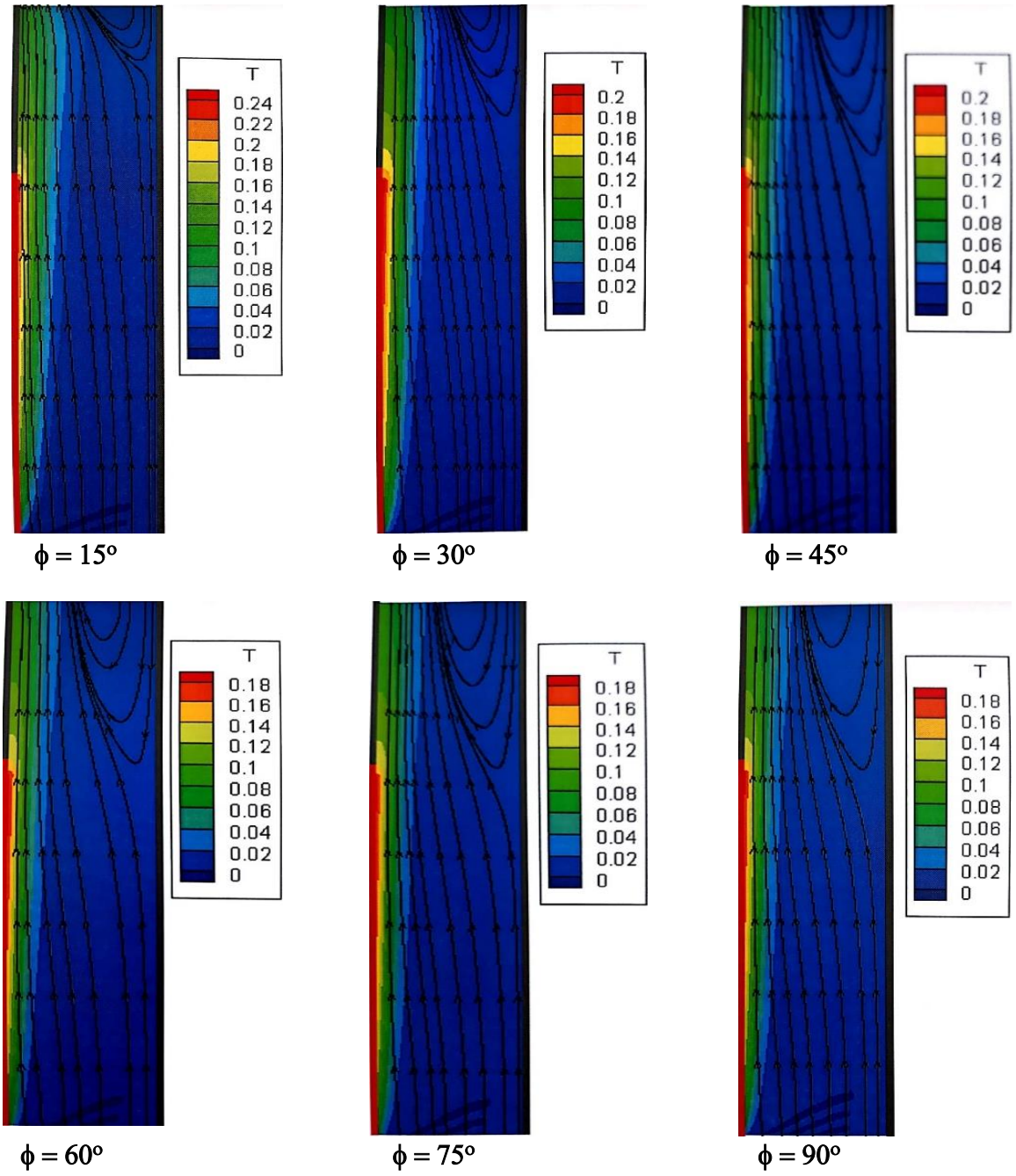

Figure 9 Streamlines and temperature fields for different inclination angles (E_{in}=0 , E_{out}=H/2 and $Ra^{*}=10^{5}$).

.

5.3 Effects of extension length

In this section, the effect of the length of the extension at the channel outlet E_{out} on the mass flow rate and on the heat transfer rate along the channel heated wall will be studied. In the following, we will fix the angle of inclination of the channel at $\phi = 28°$. This choice was made for two reasons. Firstly, open-air tests at the University of Tabuk, Saudi Arabia (latitude 28°) are in progress. These

Exp. Theo. NANOTECHNOLOGY 3 (2019) 405-426

experiments will provide more details on the actual performance of the studied system under a desert climate. Secondly, the existence of a substantial reduction in the value of the average Nusselt number for angles of inclination of less than 30° as observed by Talukdar et al. [22].

The effect of the extension on the channel performance is considered in a parametric study for an inclination angle of 28° with respect to the horizontal plane. The Variation of the ratio G/G_0 as a function of the normalized adiabatic extension E_{out}/H at the outlet of the channel for different modified Rayleigh numbers ($Ra^*=10^3$, 10^4, 10^5) is depicted in Figureure 10. It is observed that the mass flow rate ratio increases with the increase of the extension length and the modified Rayleigh number. It should be noted that increasing the extension length E_{out} from 0 to 2H increases the ratio G/G_0 by 56% at $Ra^*=10^3$, by 96% at $Ra^*=10^4$ and 153% at $Ra^*=10^5$.

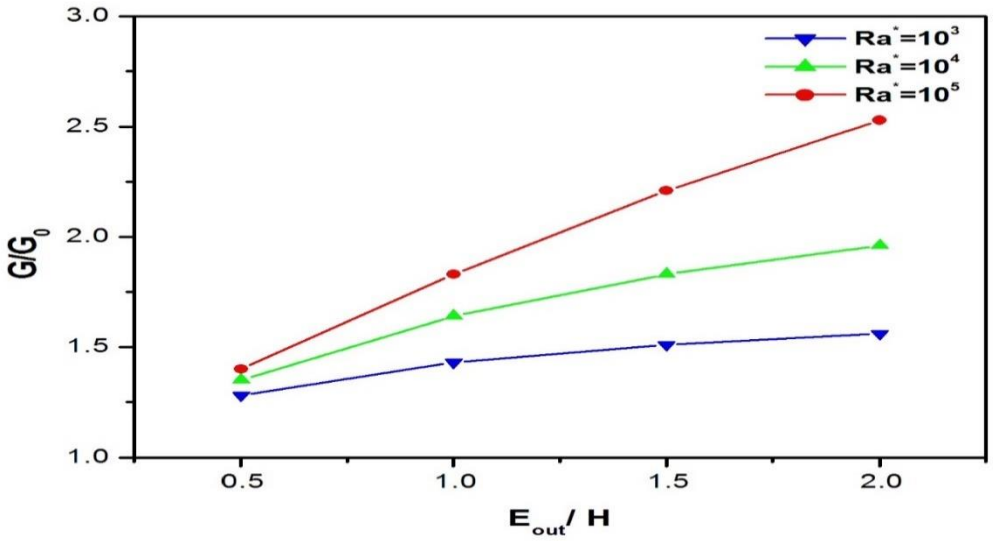

Figure 10 Variation of the ratio G/G_0 as a function of the normalized adiabatic extension at the outlet of the channel for different modified Rayleigh numbers.

Figure 11 shows the variation of the ratio Nu/Nu_0 as a function of the normalized adiabatic extension E_{out}/H at the outlet of the channel for different modified Rayleigh numbers ($Ra^*=10^3$, 10^4,10^5). It is observed that the heat transfer rate ratio increases with the increase of the extension length E_{out}. The results indicated that due to the increase in extension length from 0 to 2H, an Rayleigh numbers. However, the best rates of improvement are obtained for the low Rayleigh Nu/Nu_0 is 15% at $Ra^*=10^3$, 14% at $Ra^*=10^4$ and 12% at $Ra^*=10^5$.increase in convective heat loss is obtained for all modified numbers. Indeed, when the length of the extension goes from 0 to 2H, the rate of enhancement of the ratio

Exp. Theo. NANOTECHNOLOGY 3 (2019) 405-426

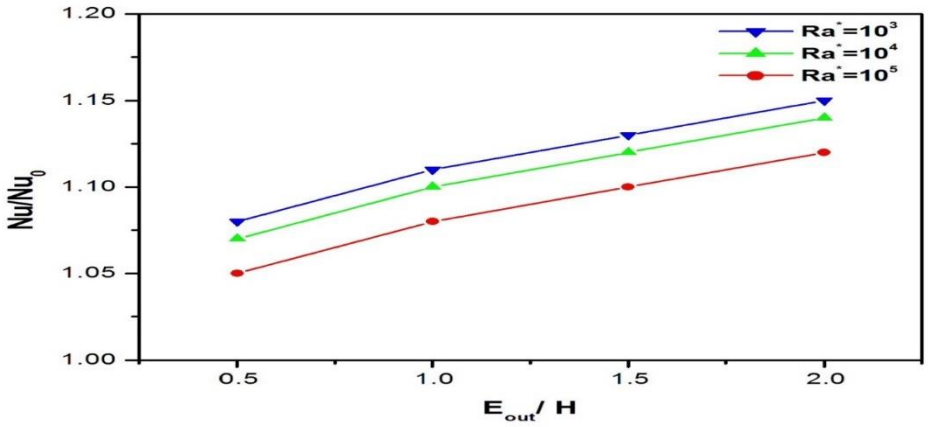

Figure 11 Variation of the ratio Nu/Nu_0 as a function of the normalized adiabatic extension at the outlet of the channel for different modified Rayleigh numbers.

To explain the heat transfer rate improvement due to the increase in extension length Eout, Figure 12 shows the streamlines and the temperature fields for different values of Eout and for a modified Rayleigh number $Ra^*=10^5$. A recirculation zone adjacent to the lower adiabatic wall is established at the outlet of the channel. The size of this vortex decreases with the increase of the length of extension until its disappearance for $E_{out} = 2H$ and the streamlines become parallel to the channel axis. The recirculation zone blocked the exit of the canal and its disappearance freed the flow. This explains the increase in the mass flow rate and consequently the improvement of the heat transfer rate in the channel.

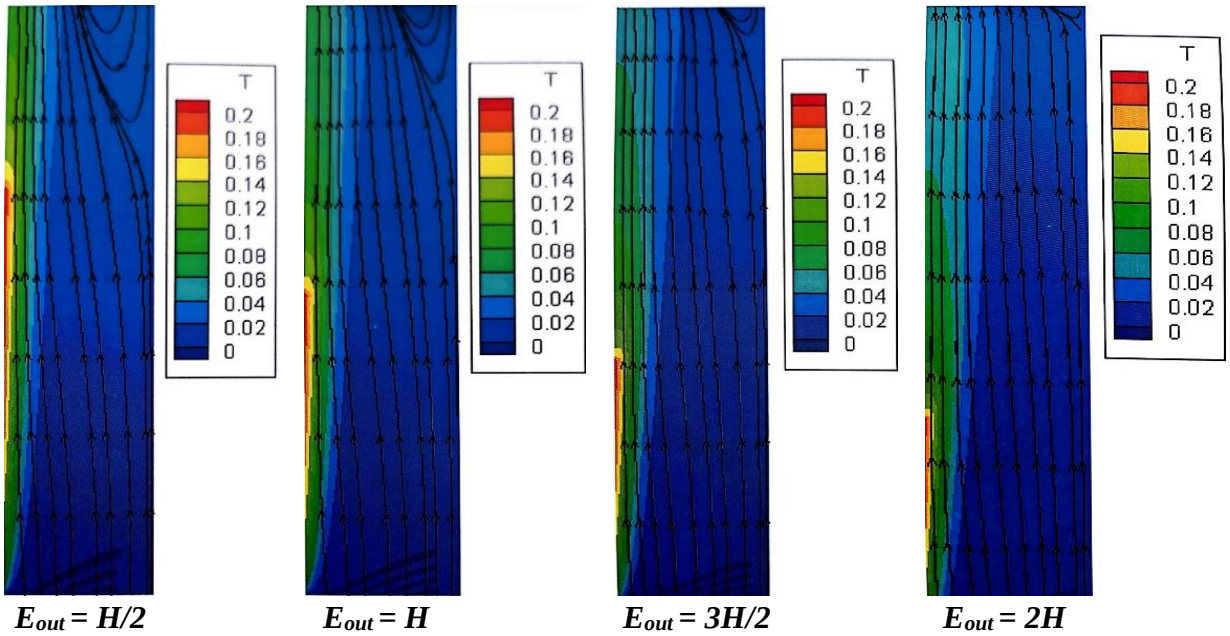

Figure 12 Streamlines and temperature fields for different lengths of the extension at the channel outlet.(E_{in}=0 and $Ra^*=10^5$).

Exp. Theo. NANOTECHNOLOGY 3 (2019) 405-426

5. CONCLUSIONS

A numerical investigation on air natural convection in an inclined channel heated asymmetrically was carried out to model the use of an inclined chimney as a passive cooling system to improve the efficiency of photovoltaic panels. At first, the effect of tilt angle on heat transfer rate and mass flow rate through a simple channel (without extensions) is studied for a range of modified Rayleigh number from 10^2 to 10^5, while keeping the other parameters fixed. The increase in the buoyancy forces leads to the increase in the mass flow rate and the heat transfer rate, thus improving the cooling of the photovoltaic cells. Significant reductions in air flow rate are noted for low angles of inclination, beyond 30^o. In order to improve both heat transfer and the mass flow rate induced by buoyancy, adiabatic extensions are introduced at the inlet and outlet of the simple channel. Results are presented in terms of mass flow rate ratio G/G_0, average Nusselt numbers ratio Nu/Nu0, streamlines and temperature fields. The simulations show that only the downstream extensions of the channel are effective in improving the performance of the channel. A parametric study is conducted to study the effect of the length of the extension at the channel outlet E_{out} on the mass flow rate and on the heat transfer rate along the channel-heated wall. The results showed that due to the increase in extension length from 0 to 2H, the G/G_0 ratio is increased by 153% at $Ra^* = 10^5$ and the Nu/Nu_0 ratio is increased by 15% at $Ra^* = 10^3$ and 12% at $Ra^* = 10^5$. This improvement is explained by the disappearance of the recirculation zone at the outlet of the channel.

ACKNOWLEDGEMENT

The authors would like to acknowledge financial support for this work, from the Deanship of Scientific research (DSR), University of Tabuk, Tabuk, Saudi Arabia, under Grant No. S-0277/1438.

Nomenclature

Ar: channel aspect ratio (Ar= H/b)
b: channel width (m)
E_{in}: extension at the inlet of the channel (m)
E_{out}: extension at the outlet of the channel (m)
g: Acceleration due to gravity (m.s-2)
G: dimensionless mass flow rate
G_0: Simple channel mass flow rate
H: channel length (m)
h_c: convective heat transfer coefficient (W.m-2.K-1)
ϕ: inclination angle (deg)
Nu: local Nusselt number
Nu_0: Nusselt number in the case of simple channel
Nu_a: average Nusselt number
p: pressure (Pa)

P: dimensionless modified pressure
P_r: Prandtl number
q: heat flux (W.m-2)
Ra: Rayleigh number
Ra*: modified Rayleigh number ($Ra^* = Ra/Ar$)
t: dimensionless time
t': time (s)
T: dimensionless temperature
u, w: velocity component along (x, z)-axis (m.s-1)
U, W: dimensionless velocity components
x, y: Cartesian coordinates (m)
X, Y: dimensionless Cartesian coordinates

Greek symbols

α thermal diffusivity (m2s-1)
β coefficient of thermal expansion (K-1)
θ temperature, (K)
λ thermal conductivity (W m-1 K-1)
μ dynamic viscosity (Kg m-1 s-1)
ν kinematic viscosity, μ/ρ (m2s-1)
ρ density (kg/m3)
Δ Difference between two values

Subscripts

0 : ambient
a: average
c: convective
in: inlet
out: outlet
w: wall

References

[1] M. Sandberg, B. Moshfegh, Renewable Energy 8 (1996) 254
[2] M. Sandberg, B. Moshfegh, Building and Environment 37 (2002) 211.
[3] E. Cuce, T. Bali, S. A. Sekucoglu, International Journal of Low-Carbon Technologies 6 (2011) 299
[4] F. Grubišić-Čabo, S. Nižetić, T. Giuseppe Marco, Transactions of FAMENA 40 (2016) 63
[5] G. He, J. Zhang, S. Hong, Solar Energy 136 (2016) 614
[6] M. Papadrakakis, V. Papadopoulos, G. Stefanou, V. Plevris, eccomas congress (2016)
[7] B. Brangeon, P. Joubert, A. Bastide, International Journal of Thermal Sciences, 95, (2015) 64

[8] R. Mazón-Hernández, et al., International Journal of Photoenergy, http://dx.doi.org/10.1155/2013/830968 Article ID 830968, 10 pages, (2013)
[9] N. Chami, A. Zoughaib, Energy Build. 42 (2010) 1267
[10] C.Popa, D.Ospir, S. Fohanno, C. Chereches, Energy Build. 50 (2012) 229
[11] C. Daverat, H. Pabiou, C. Menezo, H. Bouia, S. Xin, Exp. Therm. Fluid Sci. 44 (2013) 182
[12] R. Bassiouny, N. Korah, Energy Build. 41 (2009) 190
[13] J. K. Tonui, Y. Tripanagnostopoulos, Renewable Energy 32 (2007) 623
[14] J. K. Tonui, Y. Tripanagnostopoulos, Solar Energy 82 (2008) 1
[15] L.F.A. Azevedo, E.M. Sparrow, J. Heat Transfer 107 (1985) 893.
[16] N. Onur, M. Sivrioglu, M.K. Aktas, Heat Mass Transfer 32 (1997) 471
[17] M. Onur, M.K. Aktas, Int. Comm.Heat Mass Transfer 25 (1998) 389
[18] S. Baskaya, M.K. Aktas, N. Onur, Heat Mass Transfer 35 (1999) 273
[19] O. Manca, S. Nardini, Heat Transfer Eng. 20 (1999) 64
[20] T. S. Arun Samuel, M. Karthigai Pandian, A. Shenbagavalli, A. Arumugam, Exp. Theo. NANOTECHNOLOGY 2 (2018) 151
[21] B. Brangeon, P. Joubert, A. Bastide, International Journal of Thermal Sciences 95 (2015) 64
[22] D. Talukdar, C. Li, M. Tsubokura, International Journal of Heat and Mass Transfer 130 (2019) 83
[23] A. Habibzadeh, R. Zeighami, Journal of Experimental and Theoretical Nanotechnology Specialized Researches 1, (2017) 171
[24] A. H. Laatar, M. Benahmed, A. Belghith, P. Le Quéré, Journal of Wind Engineering and Industrial Aerodynamics 90 (2002) 617.
[25] S. Taieb, A. H. Laatar, J. Balti, International Journal of Thermal Sciences 74 (2013) 24
[26] Z. Nasri, A. H. Laatar, J. Balti, International Journal of Thermal Sciences 90 (2015)122
[27] Z. Nasri, Y. Derouich, A. H. Laatar, J. Balti, Heat Mass Transfer 54 (2018) 1511
[28] B. W. Webb, D. P. Hill, Journal of Heat Transfer 111 (1989) 649
[29] D. Talukdar, C. Li, M. Tsubokura, International Journal of Heat and Mass Transfer, 128 (2019) 794.

Exp. Theo. NANOTECHNOLOGY 3 (2019) 405-426